

## Cu<sub>2</sub>O Photosensitive Thin Films for Solar Cell Application

Ørnulf Nordset and Sean Erik Foss

Institute for Energy Technology, IFE  
Kjeller, Norway  
email: Ornulf.Nordseth@ife.no  
email: Sean.Foss@ife.no

Bengt Gunnar Svensson and Raj Kumar

University of Oslo  
Oslo, Norway  
email: b.g.svensson@fys.uio.no  
email: raj.kumar@smn.uio.no

Irinela Chilibon, Cristina Vasiliu,

Raluca Iordanescu, Laurentiu Baschir,  
Dan Savastru, Adrian Kiss and Anca Parau  
National Institute of Research and Development for  
Optoelectronics, INOE-2000  
Bucharest-Magurele, Romania  
emails: qilib@yahoo.com, icvasiliu@inoe.ro,  
iorda85@yahoo.com, baschirlaurentiu@inoe.ro,  
dsavas@inoe.ro, adrian.kiss@inoe.ro, anca.parau@inoe.ro

Laurentiu Fara

University Politehnica of Bucharest  
Bucharest, Romania  
email: lfara@renerg.pub.ro

Roxana Trusca

METAV-CD  
Bucharest, Romania

**Abstract**—Among copper oxides, Cu<sub>2</sub>O is intensively studied due to its high optical absorption coefficient and relatively good electrical properties. Copper oxide thin films properties depend on the deposition method as an effect of detailed arrangement of Cu and O atoms that induce different physical properties. Cu<sub>2</sub>O is a p-type semiconductor having a band gap sufficiently close to the optimal band gap under AM1.5 radiation spectrum, which makes it an attractive material for photovoltaic applications and solar cells. The structural and morphological properties of deposited thin films were investigated by Scanning Electron Microscopy (SEM) and Atomic Force Microscopy (AFM). The thin film thickness and optical constants were determined by Spectroscopic Ellipsometry (SE). The purpose of the paper was to study the technological possibilities of preparing high quality Cu<sub>2</sub>O thin films, used in photovoltaic applications. The sputter-deposited Cu<sub>2</sub>O thin films presented in this work show good potential as absorber layers for photovoltaic applications.

**Keywords**-copper oxide; solar cell; magnetron sputtering; SEM; AFM; ellipsometry.

### I. INTRODUCTION

In recent years, cuprous oxide (Cu<sub>2</sub>O) has been intensively studied due to its high optical absorption coefficient and favorable electrical properties. Cu<sub>2</sub>O thin films properties are depending on the deposition method, as a result of the detailed arrangement of Cu and O atoms that induce different physical properties. Several methods can be used to prepare Cu<sub>2</sub>O thin films, including thermal oxidation, chemical vapor deposition, plasma evaporation, reactive sputtering, and electrodeposition [1][2]. It has been reported that most of these synthesis methods result in a combined growth of Cu<sub>2</sub>O and CuO phases, which is

unfavorable in photovoltaic applications. Cu<sub>2</sub>O is very promising candidate for solar cell applications as it is a suitable material for photovoltaic energy conversion [2]. In this work, we analyze Cu<sub>2</sub>O thin films, deposited on SiO<sub>2</sub> and quartz substrates by magnetron sputtering. The purpose of the paper was to study the technological possibilities of preparing high-quality Cu<sub>2</sub>O thin films for photovoltaic applications.

The optical transmittances of the films show a strong dependence on the flow rate during deposition [1].

Ohajianya and Abumere [3] show that the efficiency of Cu<sub>2</sub>O/Cu solar cell increases as the thickness of the Cu<sub>2</sub>O decreases, up to a limiting thickness of 26.30 μm, after which the efficiency decreases as the thickness decreases.

This paper is organized as follow: Section I. Introduction presents the applications of cuprous oxide (Cu<sub>2</sub>O); Section II. describes the method for preparing copper oxide thin film; Section III. describes the structural investigations; Section IV. presents the results of the research, and the paper concludes in Section V.

### II. CUPROUS OXIDE THIN FILM PREPARATION METHOD

Cu<sub>2</sub>O is a p-type semiconductor having a band gap sufficiently close to the optimal band gap under AM1.5 radiation spectrum, which makes it an attractive material for photovoltaic applications and solar cells.

Cu<sub>2</sub>O thin films were deposited on 1 × 1 cm<sup>2</sup> quartz and silicon substrates by a direct current (DC) magnetron sputtering system (Semicore Triaxis). The quartz substrates were cleaned in piranha and rinsed in deionized water. The substrates were dried with nitrogen and loaded into the deposition chamber. Cu<sub>2</sub>O was deposited by reactive sputtering of Cu target (99.999%) in O<sub>2</sub>/Ar (6/49 sccm) with a substrate temperature of 400 °C. The power density was

fixed at 2.2 W/cm<sup>2</sup>, and experimentally established. During the magnetron sputtering deposition, the base pressure was kept below 3.0 x 10<sup>-7</sup> Torr and the sample stage was rotated at a constant speed of 12 rpm. The Cu<sub>2</sub>O thin films were deposited in two different thickness ~ 200 nm and ~ 500 nm with a deposition rate ~ 25 nm/min. As-grown Cu<sub>2</sub>O films were annealed at 900 °C for 3 minutes in vacuum (pressure ~10<sup>-1</sup> Torr) in order to enhance the optical and electrical properties [4].

### III. STRUCTURAL INVESTIGATIONS

The structural and morphological properties of deposited thin films were investigated by SEM and AFM. The thin film thickness and optical constants were determined by SE. Several variants of Cu<sub>2</sub>O thin film preparation have been considered, resulting in films of approximately 200 nm and 500 nm thickness.

TABLE I. SAMPLES AND DEPOSITION CONDITIONS FOR Cu<sub>2</sub>O THIN FILMS DEPOSITED BY MAGNETRON SPUTTERING

Sample name	Film deposition conditions
Sample 1	Cu <sub>2</sub> O (as-grown): deposited at 400 °C; film thickness ≅ 200 nm, on n-type Si substrate
Sample 2	Cu <sub>2</sub> O (as-grown): deposited at 400 °C; film thickness ≅ 500 nm, on n-type Si substrate
Sample 3	Cu <sub>2</sub> O (as-grown): deposited at 400 °C; film thickness ≅ 200 nm, on quartz substrate
Sample 4	Cu <sub>2</sub> O (annealed): deposited at 400 °C; film thickness ≅ 500 nm, on quartz substrate
Sample 5	Cu <sub>2</sub> O (annealed): deposited at 400 °C; film thickness ≅ 200 nm and annealed at 900 °C, 3 min in vacuum, on quartz substrate
Sample 6	Cu <sub>2</sub> O (annealed): deposited at 400 °C; film thickness ≅ 500 nm and annealed at 900 °C, 3 min in vacuum, on quartz substrate

Table I presents the experimental samples and deposition conditions for Cu<sub>2</sub>O thin films deposited by magnetron sputtering.

### IV. RESULTS

The structural and morphological properties of deposited thin films were investigated by SEM and Atomic Force Microscopy AFM. The thin film thickness and optical constants were determined by SE.

#### A. Scanning electron microscopy

SEM images of 200 nm and 500 nm film deposited on SiO<sub>2</sub> substrate are shown in Figures 1 and 2. For 200 nm films, the grain size is around 30 to 40 nm (Figure 1) and rarely more than 60 nm. For films of thickness 500 nm the grain size increased to 60 - 70 nm (Figure 2).

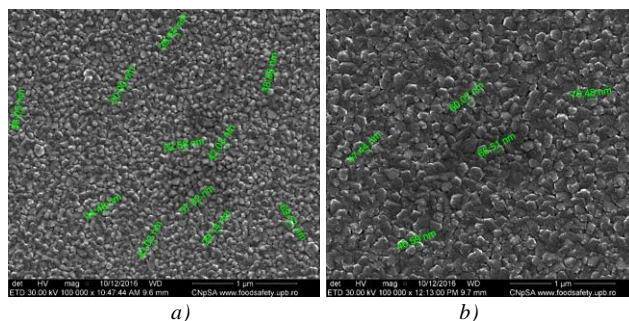


Figure 1. SEM images of a) 200 nm as-grown Cu<sub>2</sub>O thin film on Si substrate, *Sample 1* and b) SEM image of 500 nm as-grown Cu<sub>2</sub>O thin film on Si substrate, *Sample 2*.

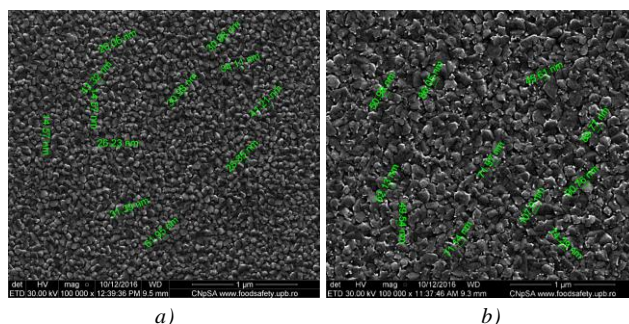


Figure 2. SEM images of a) SEM image of 200 nm as-grown Cu<sub>2</sub>O thin film on quartz substrate, *Sample 3* and b) SEM image of 500 nm as-grown Cu<sub>2</sub>O thin film on quartz substrate, *Sample 4*.

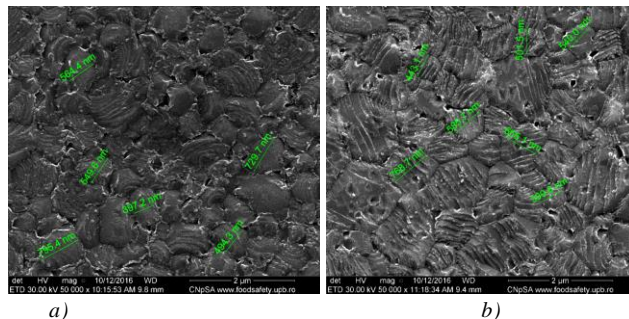


Figure 3. SEM images of a) 200 nm annealed Cu<sub>2</sub>O thin film on quartz substrate, *Sample 5* and b) 500 nm annealed Cu<sub>2</sub>O thin film on quartz substrate, *Sample 6*.

Figure 3 presents SEM images for *Sample 5* and *Sample 6*, deposited on quartz substrate. It is noticeable that for the Cu<sub>2</sub>O thin film on quartz, average grain size increases from ~70 nm for the as-grown film to ~600 nm for the annealed film [4].

The size of the grains depends on the thickness of the films deposited and the type of substrate material. For the SiO<sub>2</sub> substrate it is noticeable that the grains deposited are more uniform and smaller than the films deposited on the quartz.

For the quartz substrate, increasing the thickness of Cu<sub>2</sub>O films, from 200 nm to 500 nm, also increases grain size.

**B. Atomic force microscopy**

In order to study the effect of the deposition condition on the morphology of the Cu<sub>2</sub>O thin film, the morphologies of all samples have been analyzed using an Atomic Force Microscope (AFM), (INNOVA, Veeco Company). For the data acquisition, we used an AFM probe model RTESPA, doped with Si and for image analysis we used Scanning Probe Microscopy with special SPM Lab Analysis v.7.0 software (from Veeco Company). The scanning was made in tapping mode and the scanning speed was about 2.5 μm/s on a surface area of 10×10 μm<sup>2</sup>. The AFM images had a resolution of 512×512 pixels. For all the samples, the AFM images were performed first on 30×30 μm<sup>2</sup> area and then on the 10×10 μm<sup>2</sup> area, representing the cleanest zone of the large area.

AFM data analysis allows quantitative information to be extracted on surface roughness. A systematic description of various analytical methods used for roughness characterization can be found in [5]. The root-mean square roughness (R<sub>RMS</sub>) is defined as the standard deviation of the surface height profile from the mean height, (1).

$$R_{RMS} = \left[ \frac{1}{N} \sum_{n=1}^n (h_i - \langle h \rangle)^2 \right]^{\frac{1}{2}} \quad (1)$$

where N is the number of pixels in the image (or data points), h<sub>i</sub> is the height of the i<sup>th</sup> pixel, and h is the mean height of the image [5].

The AFM has been employed to determine the morphology, the grain size and the root mean square (RMS) surface roughness of all deposited films at 400 °C as-grown for 200 nm and 500 nm thicknesses of films, and annealed at 900 °C for 200 nm and 500 nm thicknesses of films.

The 2D and 3D AFM images of Cu<sub>2</sub>O thin films deposited at different conditions show the surface morphologies of the films (Figures 4 to 8). Generally, we found that an increase in the thickness of Cu<sub>2</sub>O films potential results in an increase of the grain size and RMS surface roughness, as shown in Table II.

TABLE II. RMS FOR Cu<sub>2</sub>O THIN FILMS

Sample name	RMS roughness [nm]
Sample 2	6.31
Sample 3	1.58
Sample 4	7.95
Sample 5	15.65
Sample 6	20.60

For the same thickness of 500 nm, the roughness on Si substrate is smaller than the roughness on quartz. Sample 6 has the greatest RMS roughness.

Generally, during the Cu<sub>2</sub>O film making, we found that an increase in film thickness and the treatment temperature

increase the grain size and implicitly the roughness of the films.

Samples 2 and 4 had similar roughness, the coating was not influenced by the two selected substrates (Si and quartz substrates). However, we notice that the coating on Si substrate (Sample 2) had more dense and compact columns, compared with Sample 4.

After the film deposition at 400 °C, it was observed the fine structure for the coatings on Samples 3 and 4, emphasized by the low roughness values (1.58 nm, respectively 7.95 nm).

The annealing at 900 °C, 3 min in vacuum led to an increase of roughness for both samples with different layers thickness deposited on quartz substrate (Samples 5 and 6).

Sample 6, with a thickness of 500 nm, after the annealing, presented the largest grains size and therefore the highest value of roughness parameter (20.60 nm).

**C. Spectroscopic ellipsometry**

Spectroscopic ellipsometry and reflectivity measurements are used for determination of Cu<sub>2</sub>O film thickness [6].

For determination of the optical properties of the Cu<sub>2</sub>O films, a layer-by-layer growth model was used as presented in Figure 9 [7]. In the calculation process, optical constants of each material in the respective layer are cited from the literature. The surface roughness is modeled by mixing the optical constants of surface material (Cu<sub>2</sub>O) and 50% air (i.e., n = 1 and k = 0) as shown in Figure 9.

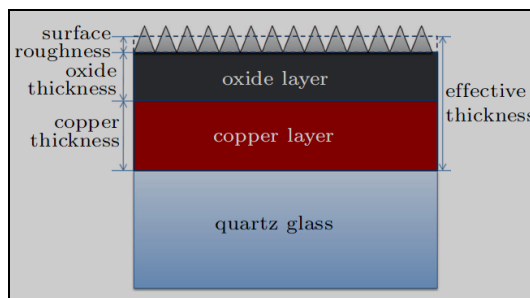


Figure 9. Schematic illustration of 3-layer model for oxidized Cu layer on quartz substrate [7].

We used the UVISSEL Spectroscopic Ellipsometer equipment from HORIBA Jobin Yvon in the spectral range 190-2100 nm [8]. All calculations were performed using DeltaPsi vs 2.6 software.

Tan Ψ and cos Δ spectra were modeled until the best fit was obtained. The model consists of a main copper oxide layer with a surface roughness layer and an interlayer layer above the (Qz/ Si) quartz / Si substrate. The Tauc - Lorentz dispersion law was used for the Cu<sub>2</sub>O layer, while the surface roughness layer was formed by one layer of Cu<sub>2</sub>O, CuO and voids. The model used is shown in Figure 10.

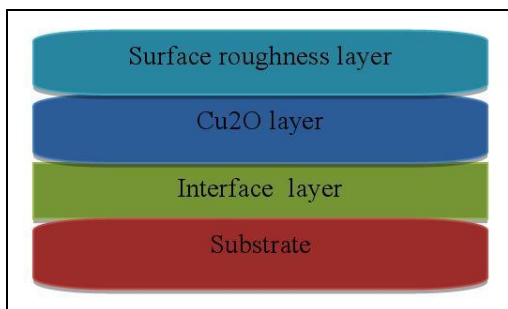


Figure 10. Model of multilayer thin copper oxide

Figure 11 presents the graphs of  $n$ ,  $k$  constants for *Sample 1*, i.e., a  $\sim 200$  nm thick  $\text{Cu}_2\text{O}$  thin film deposited by magnetron sputtering at  $400^\circ\text{C}$  on Si substrate. The model details of *Sample 1* are: Thickness  $314 \text{ nm} \pm 19,728 \text{ nm}$ ; oscillator used Tauc-Lorentz; points number 27; fit quality factor 5.120504; roughness layer  $115 \text{ nm} \pm 46.393 \text{ nm}$ ; band gap  $E_g = 2.1816$ .

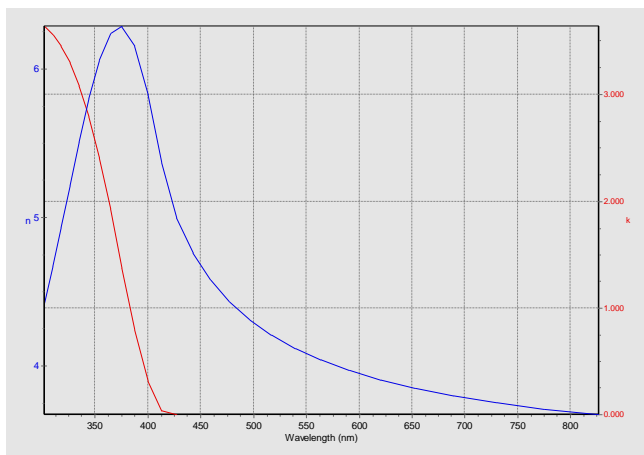


Figure 11. Graphs of  $n$  (blue curve),  $k$  (red curve) constants for *Sample 1*.

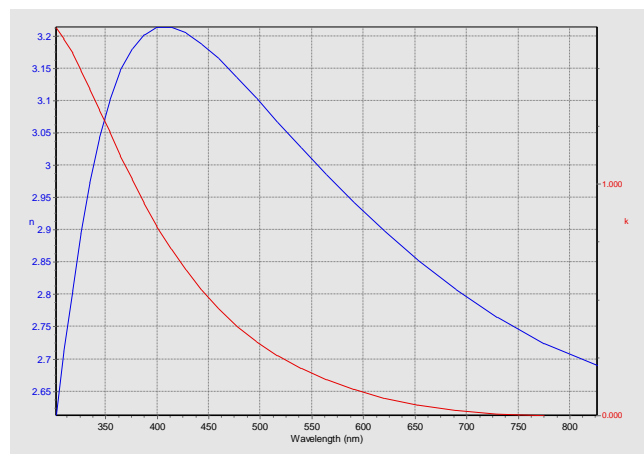


Figure 12. Graphs of  $n$  (blue curve),  $k$  (red curve) constants for *Sample 2*.

Figure 12 presents the graphs of  $n$ ,  $k$  constants for *Sample 2*, i.e., a  $\sim 500$  nm thick  $\text{Cu}_2\text{O}$  thin film deposited by magnetron sputtering at  $400^\circ\text{C}$  on Si substrate. The model

details of *Sample 2* are: Thickness  $471 \text{ nm} \pm 9.232 \text{ nm}$ ; oscillator used Tauc-Lorentz; points number 27; fit quality factor 7.929797; roughness layer  $12 \text{ nm} \pm 3.592 \text{ nm}$ ; band gap  $E_g = 1.8945$ .

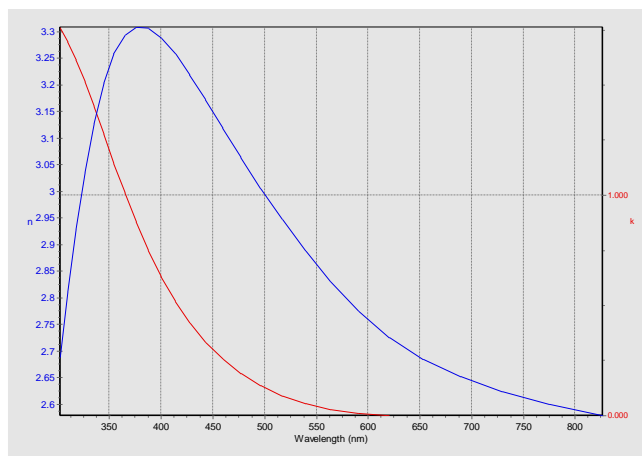


Figure 13. Graphs of  $n$  (blue curve),  $k$  (red curve) constants for *Sample 4*.

Figure 13 presents the graphs of  $n$ ,  $k$  constants for *Sample 4*, i.e., a  $\sim 500$  nm thick  $\text{Cu}_2\text{O}$  thin film deposited by magnetron sputtering at  $400^\circ\text{C}$  temperature on quartz substrate. The model details of *Sample 4* are: Thickness  $561 \text{ nm} \pm 16.858 \text{ nm}$ ; oscillator used Tauc-Lorentz; points number 27; fit quality factor 14,251030; roughness layer  $15 \text{ nm} \pm 1.663 \text{ nm}$ ; band gap  $E_g = 1.8590$ .

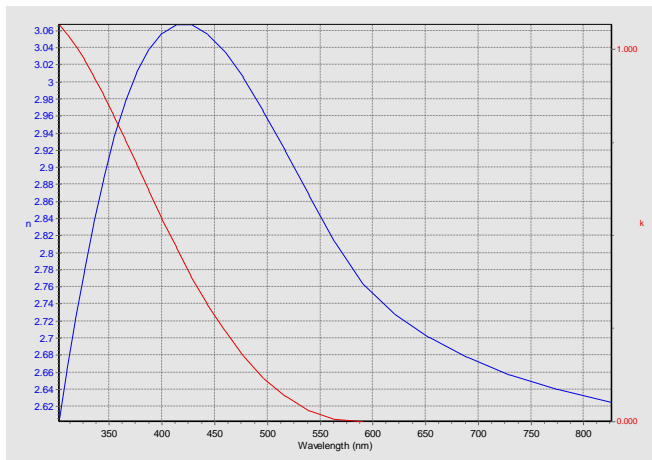


Figure 14. Graphs of  $n$  (blue curve),  $k$  (red curve) constants for *Sample 6*.

Figure 14 presents the graphs of  $n$ ,  $k$  constants for *Sample 6*, i.e., a  $\sim 500$  nm thick  $\text{Cu}_2\text{O}$  thin film deposited by magnetron sputtering at  $400^\circ\text{C}$  and treated at  $900^\circ\text{C}$  on quartz substrate. The model details of *Sample 6* are: Thickness  $590 \text{ nm} \pm 9.964 \text{ nm}$ ; oscillator used Tauc-Lorentz; points number 27; fit quality factor 10.042980; roughness layer  $21 \text{ nm} \pm 1.509 \text{ nm}$ ; band gap  $E_g = 1.6900$ .

V. CONCLUSIONS

Characterization of sputter-deposited Cu<sub>2</sub>O thin films by scanning electron microscopy and atomic force microscopy showed that the average grain size and the RMS surface roughness increases with film thickness. Spectroscopic ellipsometry measurements showed that annealing of the Cu<sub>2</sub>O film at 900°C reduces optical absorption, i.e., the extinction coefficient is reduced, presumably as a result of increased grain size [4]. In conclusion, the sputter-deposited Cu<sub>2</sub>O thin films presented in this work show good potential as an absorber layer for photovoltaic applications.

ACKNOWLEDGMENT

This work was conducted under the research project “High-performance tandem heterojunction solar cells for specific applications” (SOLHET), financially supported by the Research Council of Norway (RCN) and the Romanian Executive Agency for Higher Education, Research, Development and Innovation Funding (UEFISCDI) through the M-ERA.NET Program and 2017 Core Program, PN16-400102.

REFERENCES

- [1] F. K. Mugwang’a, P. K. Karimi, W. K. Njoroge, O. Omayio, and S. Waita, “Optical characterization of Copper Oxide thin films prepared by reactive dc magnetron sputtering for solar cell applications”, *Int. J. Thin Film Sci. Tec.*, vol. 2, no. 1, pp.15-24, 2013.
- [2] M. R. Johan, M. Shahadan, M. Suan, N. L. Hawari, H. A. Ching, “Annealing Effects on the Properties of Copper Oxide Thin Films Prepared by Chemical Deposition”, *Int. J. Electrochem. Sci.*, vol. 6, pp. 6094–6104, 2011.
- [3] C. A. Ohajianya and O. E. Abumere, “Effect Of Cuprous Oxide (Cu<sub>2</sub>O) Film Thickness On The Efficiency Of The Copper-Cuprous Oxide (Cu<sub>2</sub>O/Cu) Solar Cell”, *The International Journal of Engineering and Science (IJES)*, vol. 2, no. 5, pp. 42-47, 2013.
- [4] Ø. Nordseth, R. Kumar, K Bergum, L. Fara, S. E. Foss, H. Haug, F. Dragan, D. Crăciunescu, P. Sterian, I. Chilibon, C. Vasiliu, L. Baschir, D. Savastru, E. Momakhov, and B. G. Svensson, “Optical analysis of a ZnO/Cu<sub>2</sub>O subcell in a silicon-based tandem heterojunction solar cell”, *Green and sustainable chemistry*, vol. 7, no. 1, pp. 57-69, 2017.
- [5] J. M. Bennett and L. Mattson, “Introduction to Surface Roughness and Scattering”, *Optical Society of America*, Washington, DC, 1989.
- [6] O. Messaoudi, et al., “Correlation between optical and structural properties of copper oxide electrodeposited on ITO glass”, *J. of Alloys and Compounds*, vol. 611, pp. 142–148, 2014.
- [7] J.-B. Gong, et al. “Thickness dependence of the optical constants of oxidized copper thin films based on ellipsometry and transmittance”, *Chin. Phys. B*, vol. 23, no. 8, pp. 087802-1–087802-5, 2014.
- [8] HORIBA International Corporation [accessed August 2017] (<http://www.horiba.com/us/en/scientific/products/ellipsometers/>)

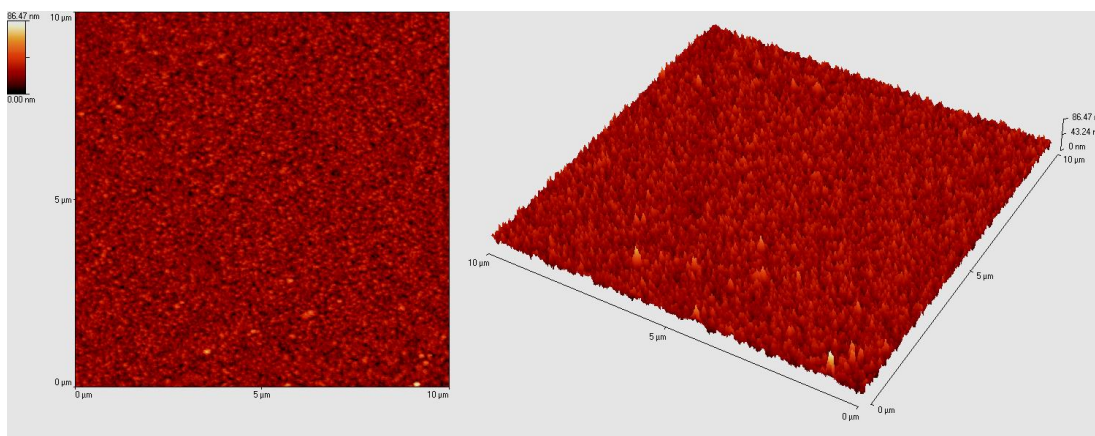


Figure 4. 2D and 3D AFM images of *Sample 2*.

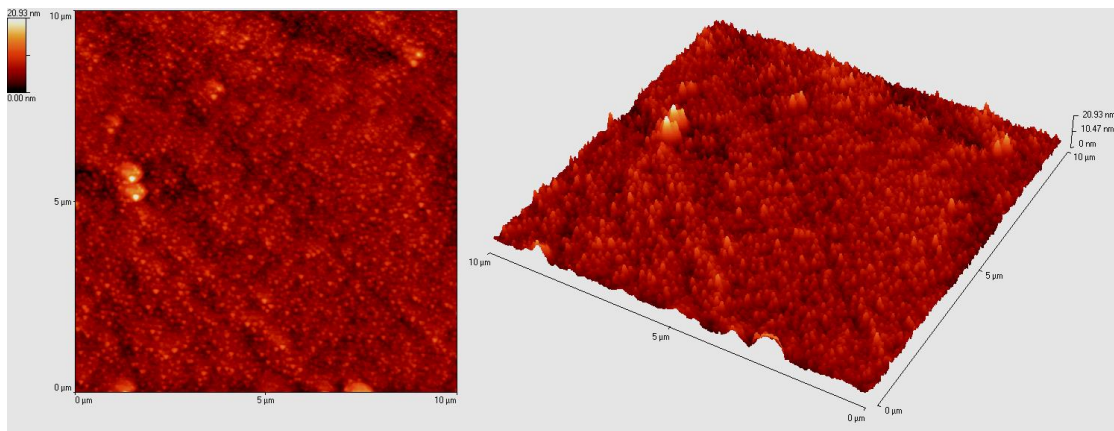


Figure 5. 2D and 3D AFM images of *Sample 3*.

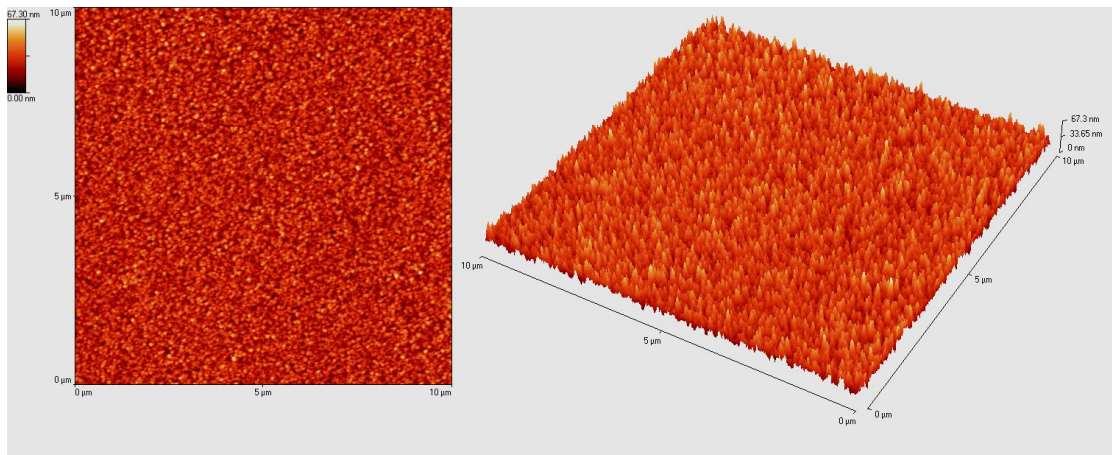


Figure 6. 2D and 3D AFM images of *Sample 4*.

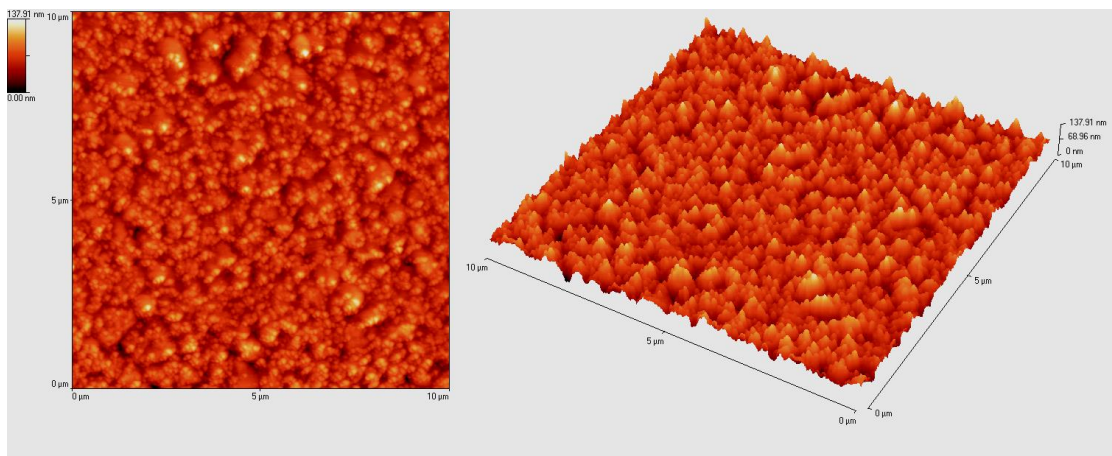


Figure 7. 2D and 3D AFM images of *Sample 5*.

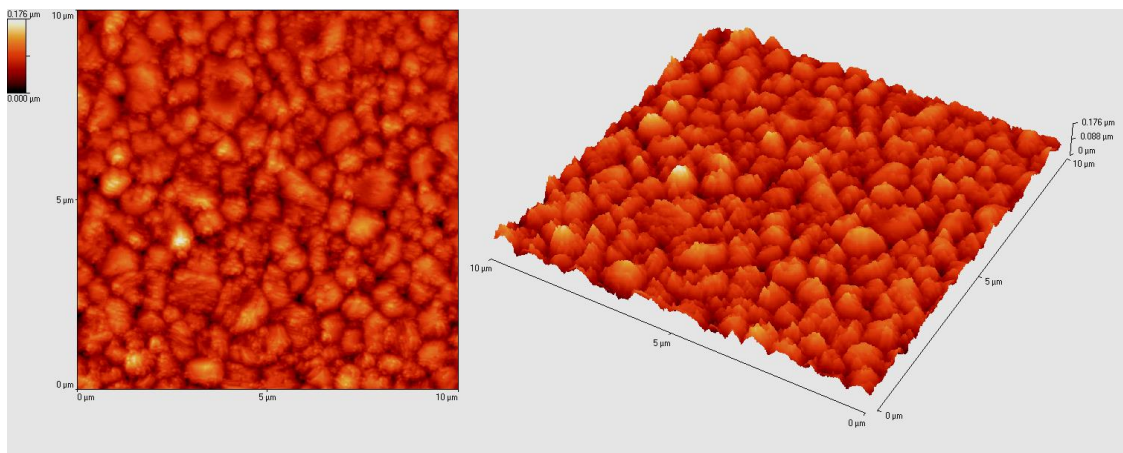


Figure 8. 2D and 3D AFM images of *Sample 6*.